The Oxygen Diffusion Coefficients of Asphalt Mixtures and Their Impacts on Mixture Aging

Xingyu Chen

Ph.D. Candidate

Department of Civil and Environmental Engineering
The Hong Kong Polytechnic University, Hung Hom, Kowloon, Hong Kong

Email: xingyu666.chen@connect.polyu.hk

Yuhong Wang, Corresponding author

Professor

Department of Civil and Environmental Engineering
The Hong Kong Polytechnic University, Hung Hom, Kowloon, Hong Kong

Email: ceyhwang@polyu.edu.hk

Yong Wen

Associate Professor

School of Highway

Chang'an University, Xi'an, Shaanxi, China

Email: wy-1026@163.com

Huailei Cheng

Ph.D.

[1]The Key Laboratory of Road and Traffic Engineering, Ministry of Education

Tongji University, Shanghai, China, 201804

[2]Department of Civil and Environmental Engineering

The Hong Kong Polytechnic University, Hung Hom, Kowloon, Hong Kong

Email: chl6218@tongji.edu.cn

Gengren Hao

Ph.D. Candidate

Department of Civil and Environmental Engineering
The Hong Kong Polytechnic University, Hung Hom, Kowloon, Hong Kong

Email: gengren.hao@connect.polyu.hk

Abstract

The oxidative aging of asphalt binder affects the long-term performance of flexible pavement. Apart from the intrinsic property of asphalt binder, binder aging in an asphalt mixture is also affected by the mixture's oxygen transport efficiency, which can be characterized by the oxygen diffusion coefficient. In this study, the diffusion coefficients (*Ds*) of compacted asphalt mixtures of different designs were determined. The same mixture samples were also aged in one dimension for a relatively long period of time. Asphalt binders from different slices of the aged specimens were extracted and recovered, and their aging states were determined. Influences of *Ds* and air void content on binder aging gradient and binder aging extent in the mixture samples were systematically examined and compared. The results indicate that, as compared to air voids, *Ds* is more closely related to the aging susceptibility of asphalt binders in asphalt mixtures. It may serve as a useful and convenient parameter in mixture design optimization, modeling and prediction of in-situ pavement aging, and quality control and quality assurance (QC/QA) in pavement construction.

Keywords:

Oxygen diffusion, asphalt aging, asphalt mixtures, aging in asphalt mixtures, aging gradient.

1. Introduction

As an organic material, asphalt binder in asphalt mixture is prone to oxidative aging (*1, 2, 3*). Aging increases the stiffness and brittleness of asphalt binder and affects the long-term performance of asphalt pavement (*4*). Therefore, the aging susceptibility of asphalt binder and asphalt mixture is one of the key concerned parameters in material characterization and an important quality characteristic in pavement quality control and quality assurance (QC/QA).

Aging-related issues of asphalt binder have been investigated in numerous studies (e.g., *5, 6, 7, 8, 9*). It is commonly believed that binder's oxidative aging only occurs at the top surface of asphalt pavements, as the surface layer is directly exposed to the atmosphere (*10, 11*). However, more recent studies including field investigations (*12, 13, 14, 15*) clearly show that asphalt binders age throughout the pavement layers. Hence, it is necessary to understand factors that affect binder aging in asphalt mixtures, the aging gradient of asphalt binders along the pavement depth, and the effects of binder aging on pavement performance. Such information is critically important in selecting right materials for the job and predicting pavement performance over time.

The extent of binder aging varies from the surface of an asphalt mixture to its core. The aging gradient of an asphalt mixture is highly dependent on its oxygen transport efficiency, which is determined by the volumetric properties of the mixture. Several pioneering studies at the Texas A&M University (*16, 17, 18, 19, 20*) investigated the issues of oxygen transport in asphalt mixtures. Assisted with X-ray computed tomography (CT) technology, Prapaitrakul (*19*) developed an oxygen transport and reaction model, where oxygen was modeled to be transported in air void (AV) channels and diffused into asphalt binder shells, and the average AV size and distance between adjacent pores were used to predict binder oxidation. Han (*17*) refined the model by including temperature and the number of air voids (AVs) in oxidation prediction. Rose (*18*) made further contributions to AV characterization and incorporated AV properties in oxidation modeling. Based on the earlier models, Han *et al.* (21) improved the asphalt oxidation model by introducing the measurement of oxygen diffusivity in modified/unmodified binders and mastics. Furthermore, Jin *et al.* (22) introduced a field factor to account for some other factors affecting the oxidative aging of asphalt binders, including oxygen path around aggregates, binder absorption, and micro cracks. In addition, an asphalt mixture morphology framework was developed and applied at the Royal Institute of Technology (KTH) to investigate the aging susceptibility of asphalt mixtures by considering aggregate gradation, asphalt content, and compaction level (23). Although these investigations provide valuable insights, the use of CT images to characterize AVs has several limits, including inadequate CT image resolution to characterize small AVs (*17*), challenges in computing algorithms to differentiate AVs from surrounding materials accurately (24), and difficulty and cost in practical implementation (*25*). Considering the limitation of X-ray CT, Rose (*18*) recommended to find alternative parameters for oxidation modeling without relying on the morphological details of AVs in asphalt mixtures.

By using embedded oxygen sensors, Wang *et al.* (*26*) and Fini A *et al*. (*27*) found that oxygen concentrations in the air underneath pavement slabs are lower than that in the atmosphere. The difference in oxygen concentration drives oxygen in the air to diffuse into deeper pavement layers. Inspired by studies (*28, 29*) on gaseous diffusions in porous media, researchers (*30*) developed a set of equipment and procedure to measure the rate of oxygen diffusion in compacted asphalt mixtures, and they also identified methods to compute the oxygen diffusion coefficients (*Ds*) of compacted asphalt mixtures. The coefficient provides an overall indication of asphalt binder's accessibility to oxygen in a mixture and the mixture's oxygen transport efficiency. Thus, apart from the intrinsic aging susceptibility of an asphalt binder, *Ds* is expected to serve as a valuable surrogate to assess the aging susceptibility of the same asphalt binder in different mixtures and to assist modeling the oxidative aging of asphalt mixture in field pavements. However, relationships between *Ds* and asphalt mixtures' aging susceptibility remain to be systematically examined.

To fill this research gap, this study aims to investigate the effects of *Ds* on the aging susceptibility of asphalt mixtures. For comparison purposes, the effects of AV content on the aging susceptibility of asphalt mixtures are also examined. A total of 32 specimens based on four mixture types were prepared for the diffusion test, and the *Ds* of different specimens were identified based on the test results. After the *Ds* was determined, all the specimens were placed into an oven at 60 °C for 21 days to simulate the long-term aging in asphalt pavements. Since *Ds* characterizes the one-dimensional oxygen diffusion in asphalt mixtures, the aging process should be created to simulate one-dimensional oxygen transport, too. Therefore, in simulated aging treatments, wax with a melting point of 80 °C was wrapped around the specimen to prevent oxygen diffusion from the sides of the specimens. After aging treatments, all the specimens were cut into five layers from top to bottom. Asphalt binder from each layer was extracted, recovered, and tested for the aging state using the Fourier transform infrared spectroscopy (FTIR) technique. The carbonyl (C=O) index derived from the FTIR test was used to characterize the aging state of the extracted asphalt binders. Variations in the aging state of asphalt binders from different layers reflect the aging gradient of the asphalt mixture along the depth profile. Correlations between *Ds* and aging gradient and between AV content and aging gradient were investigated to evaluate which parameter better predicts the aging susceptibility of compacted asphalt mixtures.

2. Materials

2.1 Aggregate and asphalt binder

Crushed granite obtained from a local quarry and neat asphalt binder with a penetration grade of 60/70 (typically PG64-16) supplied by Shell Hong Kong Limited Company were used to prepare the asphalt mixtures for testing. Table 1 shows some properties of the asphalt binder.

TABLE 1. Technical properties of asphalt binder

Properties	Unit	ASTM Method	Value
Specific gravity @ 25 °C		D 70	1.039
Softening Point, R&B	°C	D 36	46.2
Penetration @ 25 °C	0.1 mm	D 5	68
Ductility @ 25 °C	Cm	D 113	>100
Viscosity at 135 °C	mPa·s	D 4402	477.5
Flash point	°C	D 92	>232

2.2 Aggregate gradation

Asphalt mixtures with four different gradations, namely WC-10, WC-20, BC-28, and SMA-20, were designed following the Asphalt Institute Manual Series (*31*). WC, BC, and SMA are the abbreviations for wearing course, base (binder) course, and stone mastic asphalt, respectively. Fig. 1 shows the aggregate gradations of the mixtures, and the binder content for WC-10, WC-20, BC-28, and SMA-20 is designed as 6%, 5%, 4.5%, and 6.3%, respectively.

d

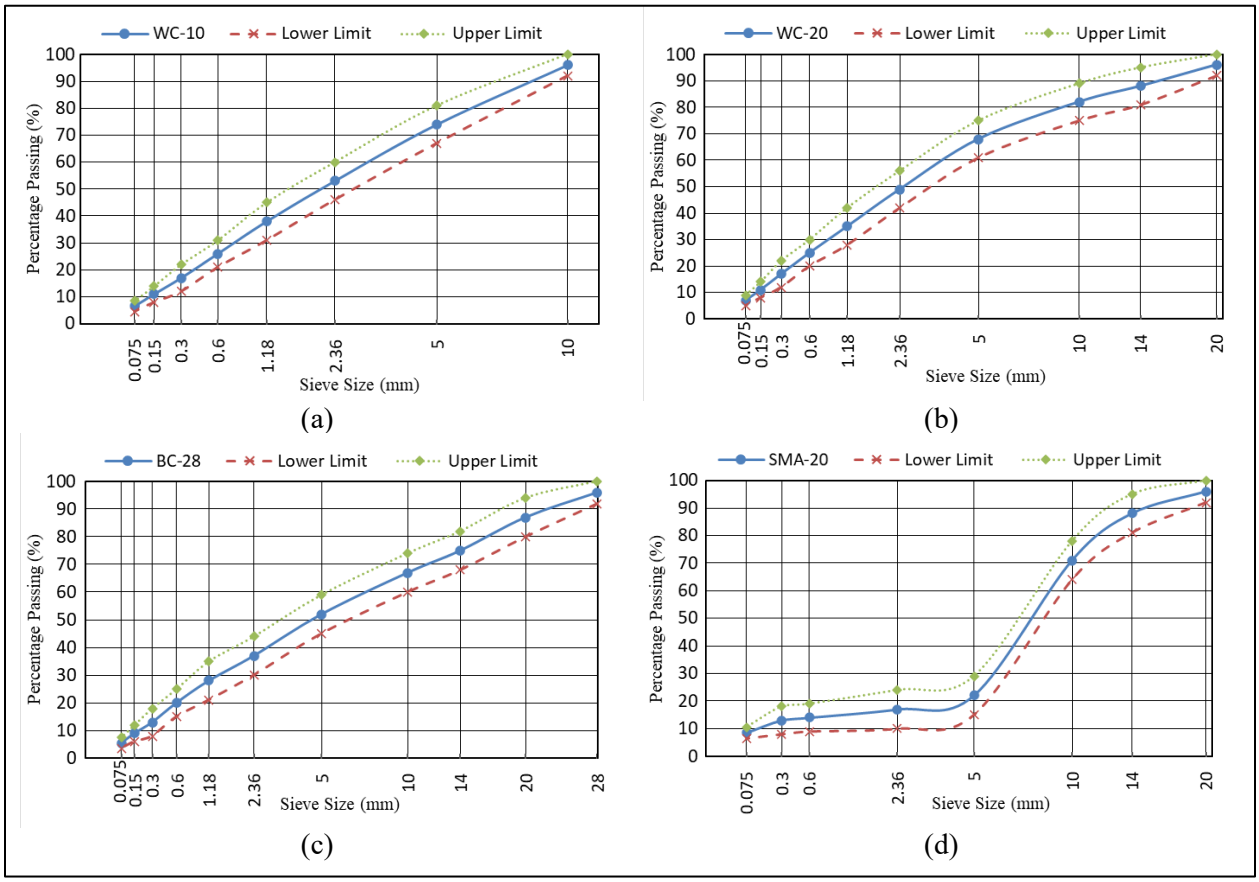

Figure 1. Aggregate gradations. (a) WC-10, (b) WC-20, (c) BC-28, (d) SMA-20.

2.3 Specimens

The schematic diagrams of the preparation process of the test specimens are shown in Figure 2. For each type of gradation, eight cylindrical specimens with a diameter of 150 mm and a height of 80 mm were compacted using the Superpave® gyratory compactor. The AVs of those eight specimens were purposely controlled to range from 3% to 10% to investigate the potential effects of AV content on the *Ds* of mixtures and the effects of AV content and *Ds* on mixtures' aging susceptibility. To reduce the effects of possible uneven compaction, the top and bottom portions of the specimens of 20 mm height were cut off and discarded. The middle part of the specimens was used for the oxygen diffusion coefficient test and subsequent aging treatment. In laboratory aging treatment, the heating temperature was set at 60 ºC to reduce the risk of binder drain down. Petersen et al. (*32*) recommended a dual oxidation mechanism: The oxygen-containing functional groups initially increase rapidly ('initial jump') and then increase slowly at a nearly constant rate (long-term aging reaction stage). In a parallel study, we have identified changes in the aging state of different asphalt binders at 60 ºC and under atmospheric pressure. The results indicate that the maximum time for the carbonyl area to exceed the 'initial jump' phase is about 20 days. Therefore, the 21-day period at 60 ºC in oven is applied in this study to simulate the long-term aging process for asphalt mixtures. The aged specimens were cut into five layers for the extraction and recovery of asphalt binders. The layers were marked as layer one to layer five from top to bottom, and the location of each layer along the vertical axis starting from the top was used to designate the layer position in the specimen, as shown in the bottom left corner of Fig. 2.

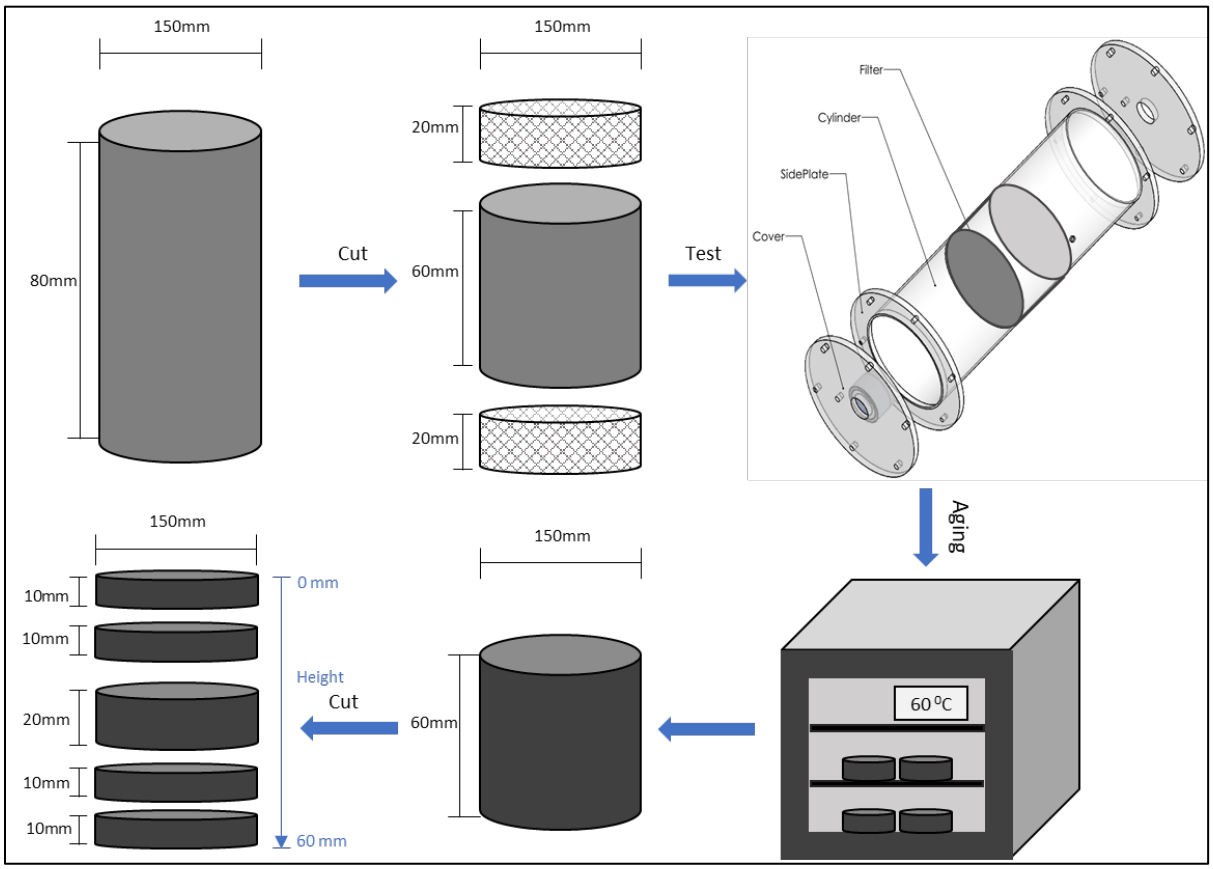

Figure 2. The schematic diagrams of specimen preparation.

3. Experimental Tests and Analysis

3.1 Experimental tests

3.1.1 Tests for the oxygen diffusion coefficient (*Ds*)

A diffusion testing system was used to test the *Ds* of compacted asphalt mixtures (*28*). The diffusion testing system consists of two components: One is the diffusion chamber, and the other is the oxygen concentration recording system. A mixture specimen is placed in the middle of the diffusion chamber. The difference in oxygen concentration drives oxygen to diffuse from one side of the specimen to the other. Time taken for the bottom and upper chambers to achieve balance in oxygen content can be used to back calculate the diffusion coefficient of the specimen. Based on previous work, the mounting system of the diffusion apparatus was redesigned in this study to provide better sealing performance. In addition, the oxygen sensor was substituted with a more stable commercial product, Apogee SO-210. The updated testing system is shown in Fig. 3.

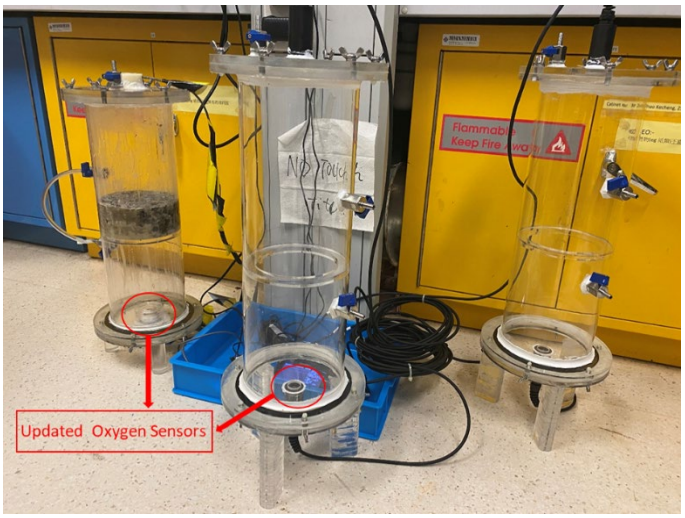

Figure 3. The diffusion testing system

The testing procedure for the determination of *Ds* is summarized as follows:

(1) Firstly, assemble the equipment and supply nitrogen to the chamber until the oxygen content approaches zero. To avoid nitrogen leakage, all the air valves and screws should be tightened. The oxygen content in the chamber is recorded continuously for 24 hours to check the sealing performance.

(2) After checking the sealing performance, open the upper cover and place the asphalt mixture specimen of a diameter of 150 mm and a height of 60 mm on the middle plate. It has been recommended to use Vaseline to seal the gap between the specimen and the chamber wall (*28*), but it is not adopted in this study since the melting point for Vaseline is lower than 60 ºC. For the convenience of implementing one-dimensional aging treatment, wax with a melting point of 80 ºC can be applied to seal the gap.

(3) The sealing of the diffusion system should be rechecked before testing. Firstly, tighten up all the screws and close the two air valves in the walls. Then, open the air valves in the upper and lower cover and blast nitrogen throughout the two opening air valves to expel oxygen in chambers until the oxygen content approaches zero. Then, close the two air valves and record the oxygen content in the chamber. If the oxygen content keeps stable in the next one hour, the apparatus is deemed to be well sealed. Otherwise, all the screws and air valves should be checked and tightened again.

(4) After checking the sealing conditions, open the two upper air valves and use an air blower to expel the nitrogen in the upper chamber until the oxygen content recovers to the same level in the air. Then, tighten the two upper air valves.

(5) During the diffusion process, the oxygen contents in the upper and lower chambers are recorded using a data logger (GL240). When the oxygen content in the upper chamber tends to be the same as the oxygen content in the lower chamber, the diffusion process is completed. However, one may also interrupt the diffusion process in the middle and use the collected data to calculate the diffusion coefficient.

Based on the test results, the *Ds* of the mixture is calculated with the proposed analytical solution, as will be introduced in section 3.2.1.

3.1.2 One-dimensional aging treatment

The oxygen diffusion coefficient was obtained based on the diffusion test in one dimension. Therefore, one-dimensional aging treatment was designed to investigate the relationship between the oxygen diffusion

coefficient and the aging susceptibility of asphalt mixtures. To achieve one-dimensional oven aging, the sides of the asphalt mixtures should be well sealed. For convenience, specimens covered with solidified wax used in the diffusion test were taken out for one-dimensional aging treatment. The specimens were aged in the oven for 21 days to simulate the long-term aging in the field, and the aging temperature was set as 60 °C to avoid wax melting since the melting point of the wax product is 80 °C. Furthermore, elastic gauze was wrapped around the mixture to prevent the wax from peeling off the specimen. Under this condition, oxygen can only transport in the mixture samples through the vertical direction, and the aging treatment setup in the oven is shown in Fig. 4. After aging treatment, the specimen was immediately wrapped in a vacuum bag to prevent further aging in the air, as shown in the left corner of Fig.4.

Figure 4. One-dimensional oven aging

3.1.3 Binder extraction and recovery

Dichloromethane was used as the extraction solvent. Asphalt binders were extracted and recovered from loose mixtures before compaction. The aging states of binders in the loose mixtures serve as a baseline to evaluate binder changes after long-term aging treatment. As introduced in Fig. 2, the aged, compacted mixture specimen was cut into five layers. The surrounded part of around 50 mm was discarded for each layer, and the central part was crushed and soaked in dichloromethane for one hour to dissolve the asphalt binder. The filtered solution of 100 ml was placed into a tube for centrifugation at 3,500 rpm for 20 minutes to remove the fine particles further. Generally, the centrifuged solution is processed in a rotary evaporator to distill the dichloromethane solvent. However, this method is not suitable in this study because the extracted asphalt binder from each layer is too little to be poured out from the flask of a rotary evaporator. Therefore, a novel approach was developed to recover the asphalt binder. As shown in Fig. 5, a customized oven equipped with a chamber filled with nitrogen was used to evaporate the dichloromethane. The centrifuged solution was placed into the chamber covered with silicon paper and slightly heated at 40 °C for one hour to evaporate most of the dichloromethane. Then, the chamber temperature was raised to 60 °C for 30 mins to recover the asphalt binders, and the recovered binder is shown in the corner of Fig. 5. To check whether the dichloromethane was thoroughly removed, the infrared spectrum of the recovered binder was examined, as shown in Fig. 6. No obvious characteristic peaks correspond to dichloromethane at 703^{-1}, 731^{-1}, and 1264^{-1}, indicating that dichloromethane is thoroughly removed.

Figure 5. Customized oven and the recovered asphalt binder

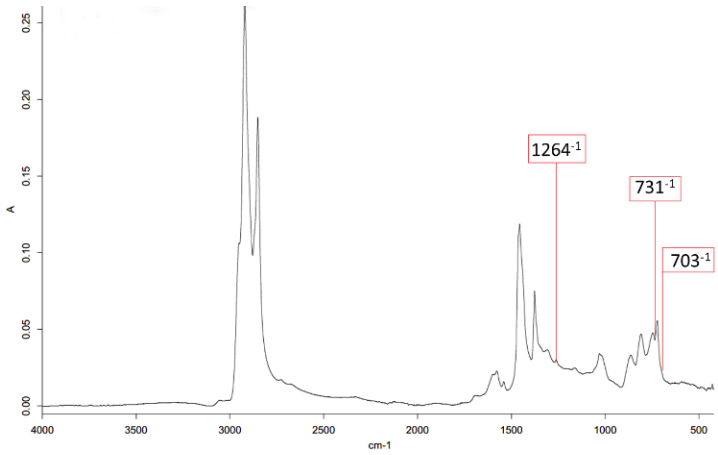

Figure 6. The infrared spectra of the extracted asphalt binder

3.1.4 Examination of the samples using FTIR

The aging states of the specimens were examined using a PerkinElmer FTIR spectrometer. The measured wavelength was set from 600 to 4000 cm^{-1} at a resolution of 4 cm^{-1}, and a baseline correction was performed for each specimen when interpreting the FTIR results. All the specimens were scanned 32 times under the attenuated total reflectance (ATR) mode, and the average results of the 32 scannings were used for analysis. Furthermore, five replicate samples were tested for each specimen, and the average result was used to represent the aging state of the recovered asphalt binder. Therefore, the actual aging states of the binders can be confidently obtained.

3.2 Analysis of experimental results

3.2.1 Determination of the oxygen diffusion coefficient (*Ds*)

Wen and Wang (*28*) introduced the computational methods to identify the oxygen diffusion coefficient D_s using the recorded oxygen contents in the two chambers, and the detailed methodology was not repeated in this article. Fig. 7 shows the sketch of the diffusion system. For easy reference, the analytical solution

without considering oxygen consumption in compacted asphalt mixtures is shown as follows, and D_s can be identified using the Solver Tool in Excel.

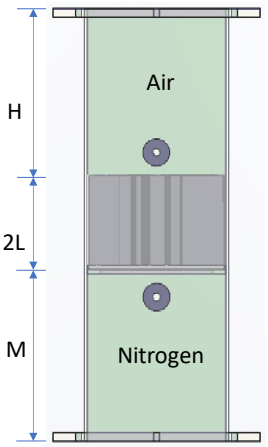

Figure 7. Dimensions in the diffusion system

$$\gamma = \frac{H}{M},\ \beta = \frac{H}{L\varepsilon},\ \tau = \frac{D_s t}{L^2 \varepsilon} \quad (1)$$

$$\alpha_1 = \left[\frac{1}{2\beta}(1+\gamma) - \frac{1}{3\beta^2}(\gamma^2 - \gamma + 1) + \frac{2}{45\beta^3}(4\gamma^3 - 3\gamma^2 - 3\gamma + 4)\right]^{1/2} \quad (2)$$

For the upper chamber, $A = -\frac{\gamma}{\beta^2} - \frac{\alpha_1^2}{\gamma}$ (3)

For the lower chamber, $A = \left[\alpha_1^4 + \frac{\gamma^2}{\beta^4} + (1+\gamma^2)\left(\frac{\alpha_1}{\beta}\right)^2\right]^{1/2}$ (4)

$$B = \alpha_1^4 \frac{\beta}{\gamma} + \alpha_1^2\left(\frac{1}{\beta\gamma} + \frac{\gamma}{\beta} + \frac{1}{2\gamma} + \frac{1}{2}\right) + \frac{\gamma}{\beta^3} + \frac{\gamma}{2\beta^2} + \frac{1}{2\beta^2} \quad (5)$$

$$C(t) = C_{s0}\left[1/\left(1 + \frac{1}{\gamma} + \frac{2}{\beta}\right) - \frac{A}{B}e^{-\alpha_1^2 \tau}\right] - C_{r0} \quad (6)$$

Where γ, β, and τ are intermediate variables, *Ds* is the diffusion coefficient to be determined, α_1, A and B are the calculation factors, H is the height of the upper chamber, M is the height of the lower chamber, ε is the porosity of compacted asphalt mixtures, C_{s0} is the initial oxygen concentration of the upper chamber, C_{r0} is the initial oxygen concentration of the lower chamber, and $C(t)$ is the analytical solution of the oxygen concentration changed with diffusion time.

3.2.2 Determination of the chemical aging indicator

FTIR results help reveal changes in the aging state of asphalt binders through changes in characteristic functional groups such as carboxylic acids, ketones, and sulfoxides (*33*). Two methods are commonly recommended to analyze the FTIR results in existing asphalt binder aging studies. One is to use the peak absorbance of ketone at around 1695 cm^{-1} (*34*) as an indicator of aging, and the other one is to use the carbonyl (C=O) index (*34, 35, 36*) as an aging indicator, as shown in Eq. 7 and Eq. 8. Considering the variation of experiments, the carbonyl index based on peak areas is more robust than the aging index only

using the peak value of ketone. Therefore, the carbonyl index is chosen in this study to represent the aging state of asphalt binders.

$$\text{Carbonyl index: } I_{C=O} = AR_{1,700}/\sum AR \quad (7)$$

$$\sum AR = AR_{1,700} + AR_{1,600} + AR_{1,460} + AR_{1,376} + AR_{1,030} + AR_{864} + AR_{814} + AR_{743} + AR_{724} + AR_{(2953,2923,2862)} \quad (8)$$

Where $AR_{1,700}$ is the integrated area for carbonyl groups from 1,650 to 1,820 cm^{-1}, and $AR_{1,600}$, $AR_{1,460}$, $AR_{1,376}$, AR_{864}, AR_{814}, AR_{743}, AR_{724}, $AR_{(2953,2923,2862)}$ are the band areas for those functional groups that remain relatively stable during the aging process.

4. Results and discussion

4.1 Oxygen diffusion coefficients (*Ds*)

Fig. 8 shows changes in the measured and analytical solution of oxygen concentrations with diffusion time. The upper data serials in the figures represent oxygen concentrations in the upper air chamber, and the lower data serials refer to oxygen concentrations in the lower air chamber. Driven by the difference in oxygen concentration in the upper and lower chambers, oxygen diffuses from the upper chamber into the lower one and finally tends to achieve a balance. The longer time for the diffusion system to achieve a steady state, the smaller the *Ds* is. Testing results indicate that most specimens can arrive at a steady state in a few days, but several specimens need more than one month to reach a steady state. Time to reach the steady state is apparently dependent on the volumetric properties of asphalt mixtures.

When the testing period is too long, the leaking effect of the equipment can no longer be ignored. An example is shown in Fig. 8 (w), where the oxygen concentration in the upper air chamber is nearly unchanged whereas the oxygen concentration in the lower chamber is gradually increased. This is caused by the extremely low oxygen transportation efficiency of the sample. As a result, the rate of oxygen diffusing from the upper chamber into the lower one is even lower than the rate of oxygen leaking into the diffusion chambers. Therefore, to control the leaking effects on the computational accuracy of Ds, a failure criteria (C_f) for the diffusion test is proposed, as shown in Eq. 9. In the equation, C_f reflects the leaking level of the diffusion test, and a higher C_f means that leaking is more severe. Based on the test results of this study, it is recommended to limit the value of C_f to be within 2 %.

$$C_f = \left(C_{sf} + C_{rf}\right) - \left(C_{s0} + C_{r0}\right) \quad (9)$$

Where, C_f is the indicator of the system leaking, C_{s0} is the initial oxygen concentration of the upper chamber, C_{r0} is the initial oxygen concentration of the lower chamber, C_{sf} is final oxygen concentration of the upper chamber, and C_{rf} is the final oxygen concentration of the lower chamber.

Based on the evaluation of leaking, three specimens for WC-10 and SMA-20 and two specimens for WC-20 and BC-28 were abandoned. The common characterization of those specimens is their very low *Ds*. At very low *Ds*, because it takes a long time for the two chambers to reach equilibrium and leaking problem may interfere the results, it is not recommended to directly provide a *Ds* value for such a mixture. Instead, it is suggested to label a mixture with *Ds* less than a certain value instead of giving an accurate number. On

the other hand, the diffusion testing system may be further upgraded to control leaking so that mixture samples with very low air voids can be tested as well.

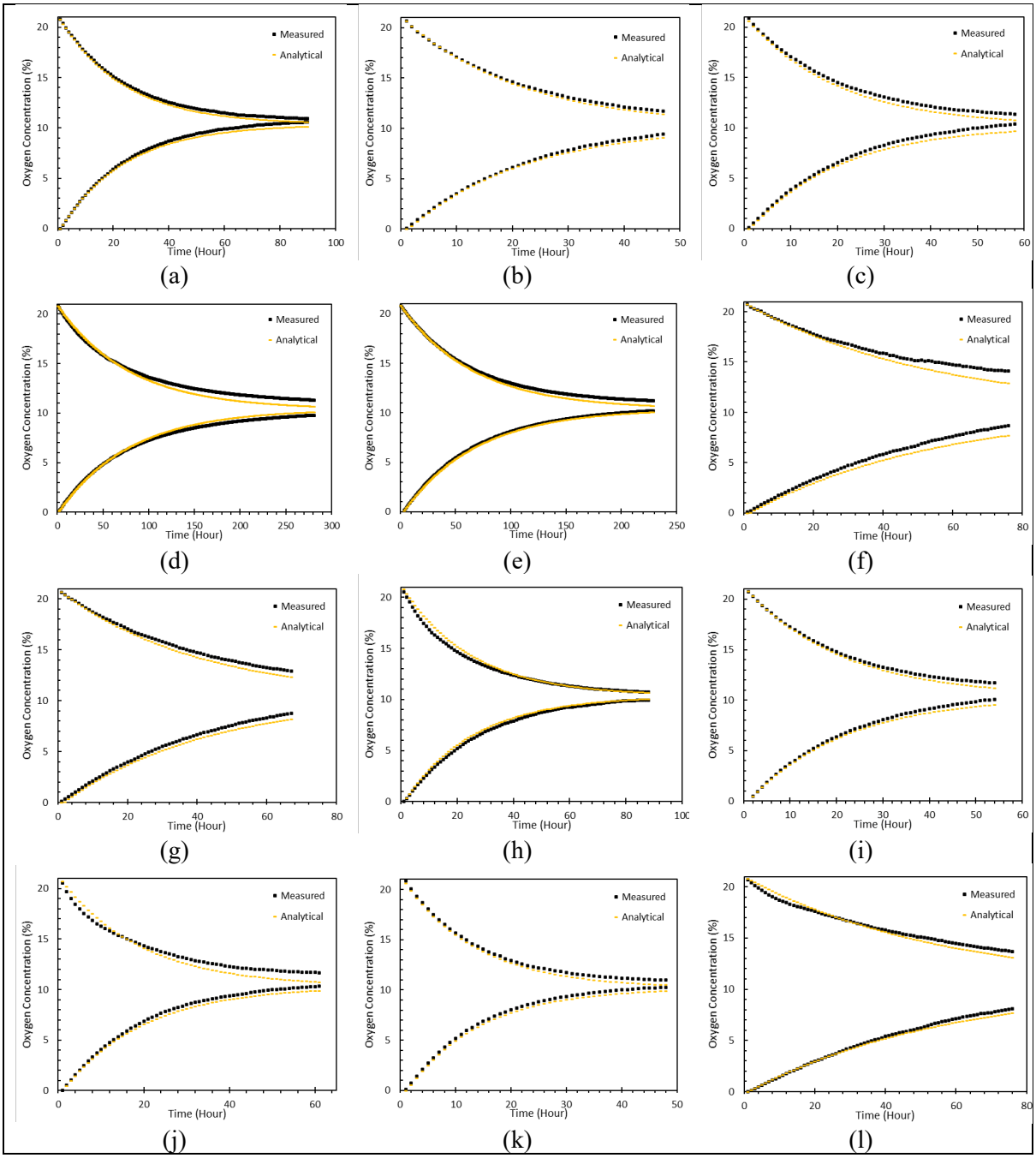

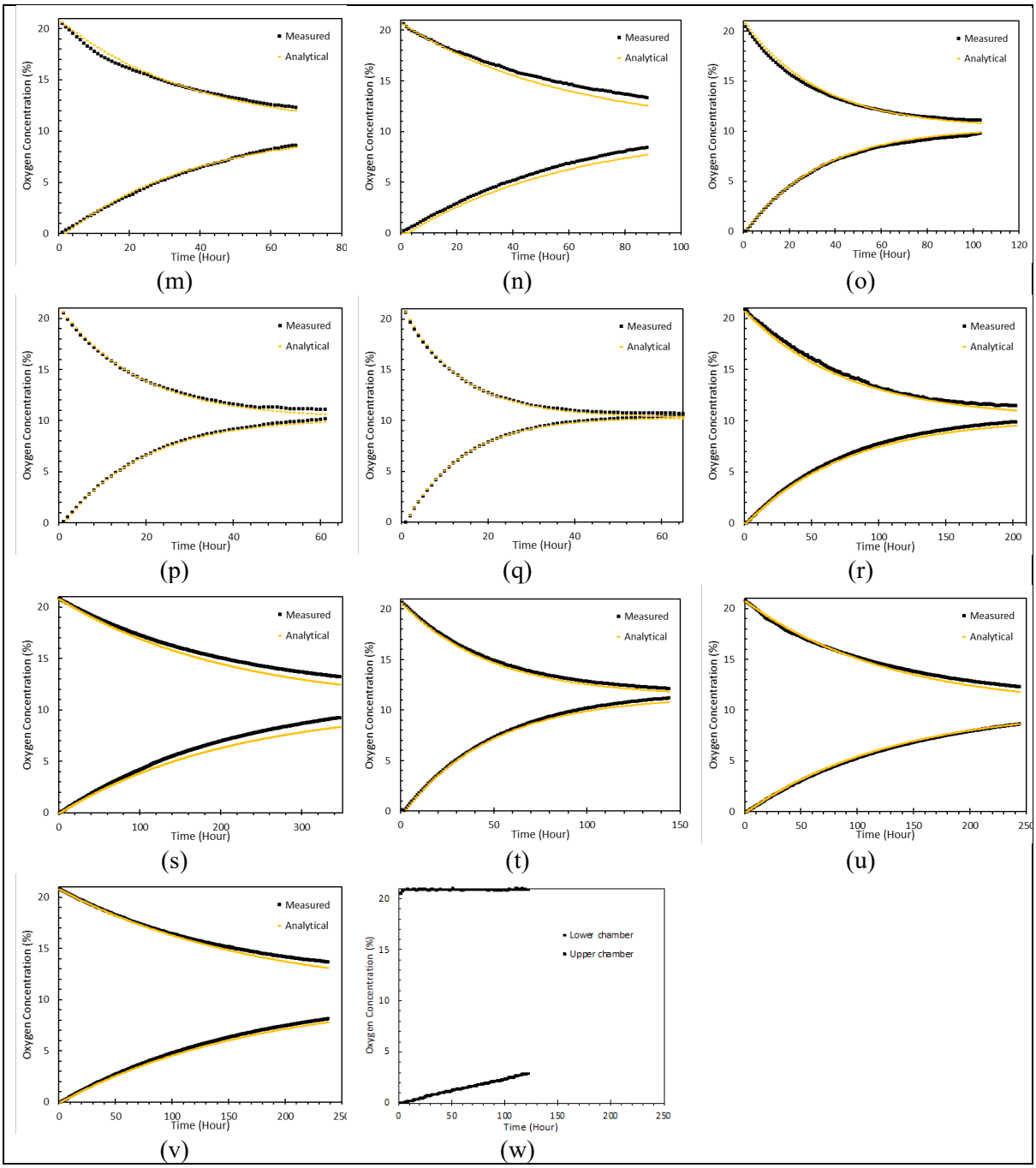

Figure 8. Results for diffusion test: (a) WC-10-1; (b) WC-10-2; (c) WC-10-3; (d) WC-10-4; (e) WC-10-5; (f) WC-20-1; (g) WC-20-2; (h) WC-20-3; (i) WC-20-4; (j) WC-20-5; (k) WC-20-6; (l) BC-28-1; (m) BC-28-2; (n) BC-28-3; (o) BC-28-4; (p) BC-28-5; (q) BC-28-6; (r) SMA-20-1; (s) SMA-20-2; (t) SMA-20-3; (u) SMA-20-4; (v) SMA-20-5; (w) SMA-20-6.

Based on data from the oxygen diffusion process shown in Fig. 8, the *Ds* of each specimen can be calculated. Table 2 presents the calculated *Ds* for each specimen and the corresponding AV content. It is noteworthy that no direct relationship exists between the *Ds* value and the AV content for different asphalt mixtures. For instance, the AV contents for WC-20-4, SMA-20-2, and BC-28-5 are all around 6%, but differences in

their *Ds* values are close to ten times. This implies that mix design plays an important role in oxygen transport in asphalt mixtures. On the other hand, for mixtures of the same gradation, the trend is quite clear—Ds increases with rising AV content. The relationships between *Ds* and AV content are shown in Fig. 9. Power functions are used to fit the *Ds* and AV content for mixtures with the same gradation, and the results are shown as Eq. 10 to Eq. 13. Satisfactory regression results support using a general function (Eq. 14) to depict the relationship between the *Ds* value and AV content of a compacted asphalt mixture.

TABLE 2. The air voids and *Ds* for each specimen

Specimen	Air voids (%)	*Ds* (cm^2/s)	Specimen	Air voids (%)	*Ds* (cm^2/s)
WC-10-1	8.8	7.48E-04	SMA-20-1	8.0	2.60E-04
WC-10-2	8.9	8.25E-04	SMA-20-2	6.0	9.27E-05
WC-10-3	9.2	8.87E-04	SMA-20-3	8.4	3.75E-04
WC-10-4	5.1	2.22E-04	SMA-20-4	7.5	1.47E-04
WC-10-5	5.5	2.64E-04	SMA-20-5	6.8	1.09E-04
WC-20-1	3.2	3.23E-04	BC-28-1	3.8	3.10E-04
WC-20-2	4.9	4.23E-04	BC-28-2	4.6	4.65E-04
WC-20-3	5.9	7.04E-04	BC-28-3	5.0	5.00E-04
WC-20-4	6.1	8.30E-04	BC-28-4	5.2	5.29E-04
WC-20-5	7.5	9.26E-04	BC-28-5	6.0	9.60E-04
WC-20-6	8.0	1.31E-03	BC-28-6	7.1	1.33E-03

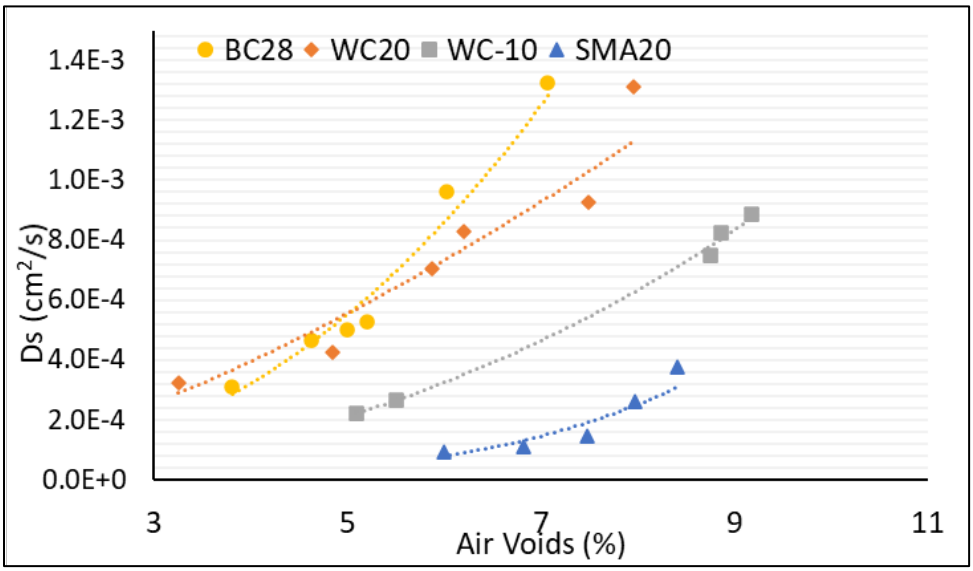

Figure 9. Relationship between air voids and *Ds*

$$\text{WC-10:} \quad Ds = 5E\text{-}6\ \varepsilon^{2.3289} \quad R^2 = 0.9956 \qquad (10)$$

$$\text{WC-20:} \quad Ds = 5E\text{-}5\ \varepsilon^{1.5279} \quad R^2 = 0.9143 \qquad (11)$$

$$\text{BC-28:} \quad Ds = 1E\text{-}5\ \varepsilon^{2.4338} \quad R^2 = 0.9774 \qquad (12)$$

SMA-20: $Ds = 5E\text{-}8\ \varepsilon^{4.1285}$ $R^2 = 0.9133$ (13)

$$Ds = K_1 \cdot \varepsilon^{k}{}_2 \quad (14)$$

Where Ds is the oxygen diffusion coefficient, ε is the AV content, and K_1 and K_2 are the fitting parameters.

Moreover, the unique curves for different asphalt mixture types in Fig. 9 suggest that the oxygen diffusion coefficient is also related to other volumetric properties, including the gradation and the nominal maximum aggregate size of the mixture. For instance, both WC-10 and WC-20 belong to the wearing course, but the oxygen diffusion coefficient of WC-20 is quite higher than that for WC-10 at the same AV level. The nominal maximum aggregate size seemingly plays a positive role in determining the oxygen diffusion coefficient. Conversely, SMA-20 and WC-20 have the same nominal maximum aggregate size, but the oxygen diffusion coefficient of SMA-20 is much smaller than that of WC-20 and even smaller than that of WC-10. Apparently, difference in D_S is affected by gradation characteristics. The gap gradation with high binder content, such as SMA-20, reduces the inter-connected pores in asphalt mixtures; therefore, oxygen transport in the SMA mixtures is relatively slow.

4.2 *Ds* and the aging gradient in asphalt mixtures

Does *Ds* affect the aging susceptibility of compacted asphalt mixtures? To answer this question, relationships between *Ds* and the aging gradients of the asphalt mixture samples were investigated. The band area of each functional group listed in Eq. 8 was measured using a commercial FTIR analysis software, OPUS. After deducting the integrated area of carbonyl formed in the mixing process (i.e., excluding the short-term aging effect), the carbonyl index of binder in each layer due to simulated long-term aging was calculated. Fig. 10 reveals the distribution of the carbonyl index from the top to the bottom layer for different mixtures. In the figure, the horizontal axis refers to the position of each layer in Fig. 2. For instance, the heights for layer-one and layer-five are 5 mm and 55 mm, respectively.

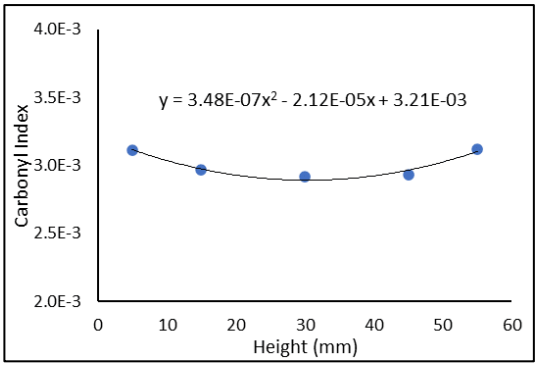

(a)

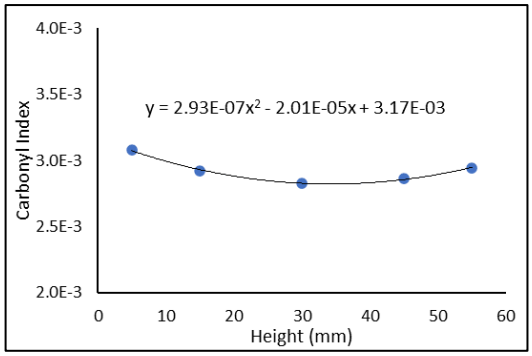

(b)

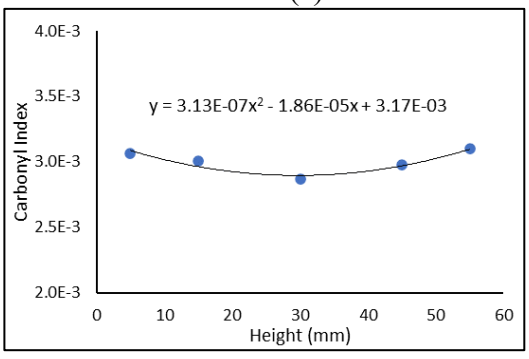

(c)

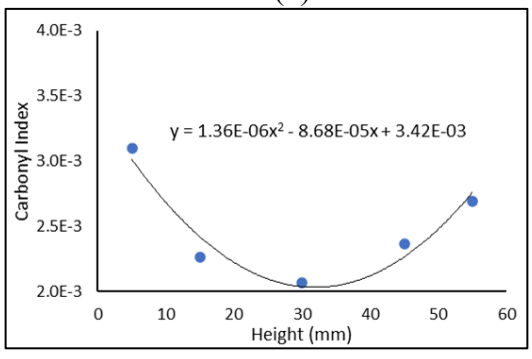

(d)

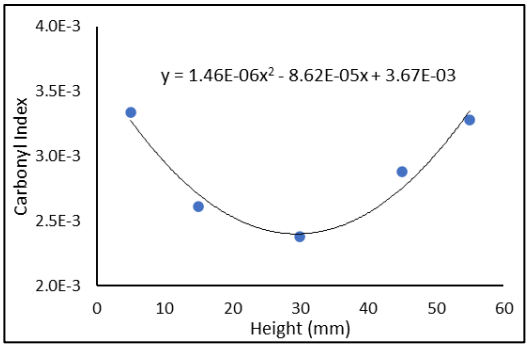
y = 1.46E-06x² - 8.62E-05x + 3.67E-03
Carbonyl Index
Height (mm)

(e)

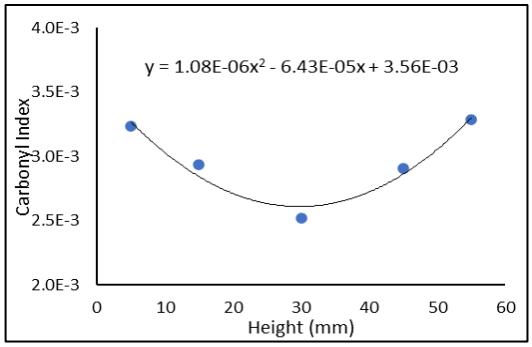
y = 1.08E-06x² - 6.43E-05x + 3.56E-03
Carbonyl Index
Height (mm)

(f)

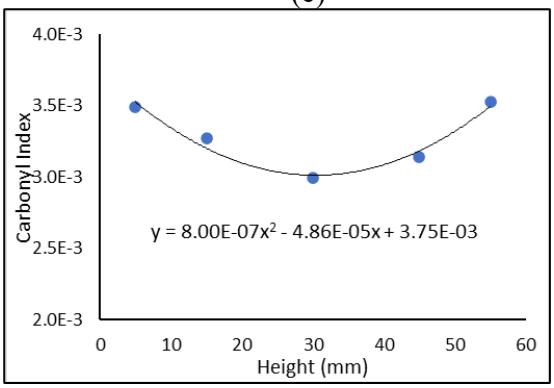
y = 8.00E-07x² - 4.86E-05x + 3.75E-03
Carbonyl Index
Height (mm)

(g)

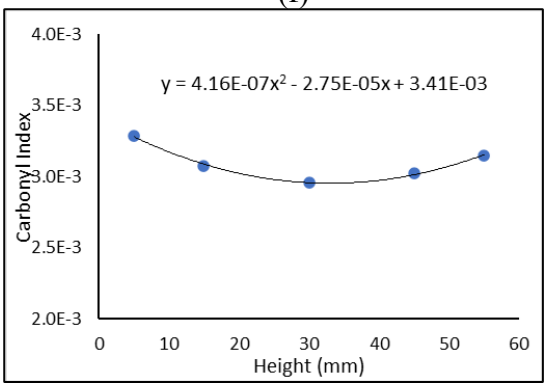
y = 4.16E-07x² - 2.75E-05x + 3.41E-03
Carbonyl Index
Height (mm)

(h)

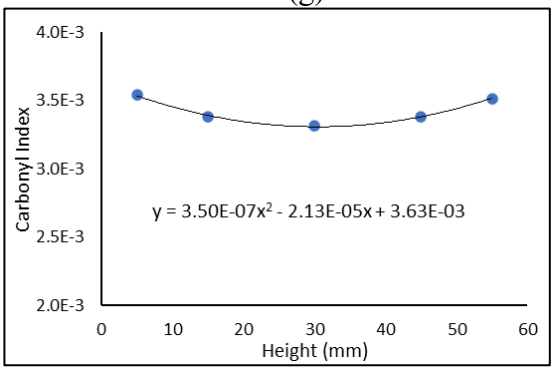
y = 3.50E-07x² - 2.13E-05x + 3.63E-03
Carbonyl Index
Height (mm)

(i)

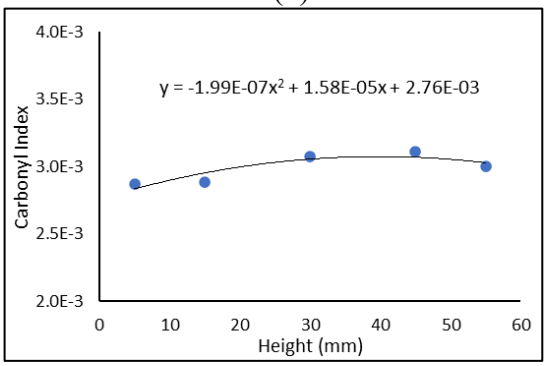
y = -1.99E-07x² + 1.58E-05x + 2.76E-03
Carbonyl Index
Height (mm)

(j)

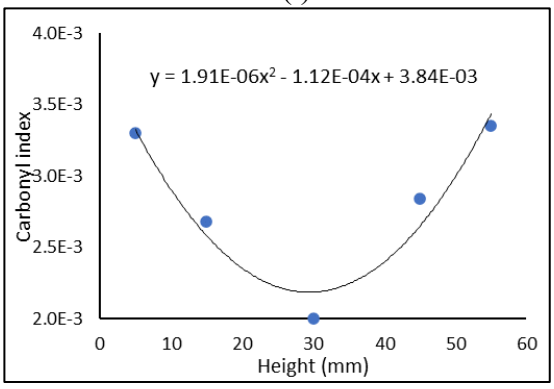
y = 1.91E-06x² - 1.12E-04x + 3.84E-03
Carbonyl index
Height (mm)

(k)

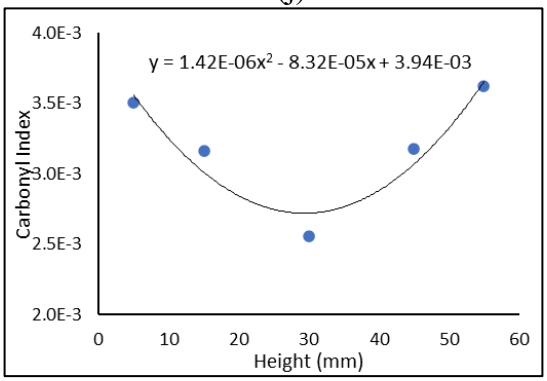
y = 1.42E-06x² - 8.32E-05x + 3.94E-03
Carbonyl Index
Height (mm)

(l)

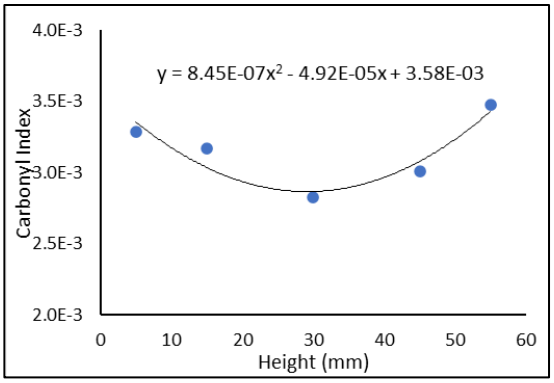

(m)

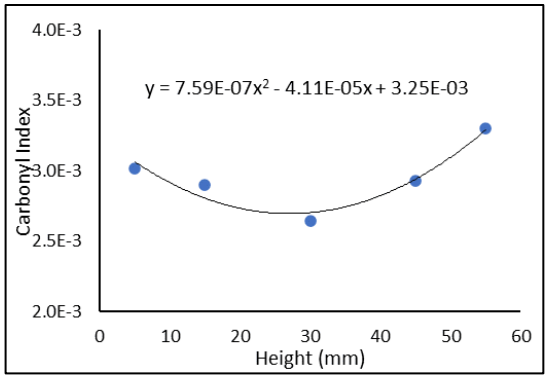

(n)

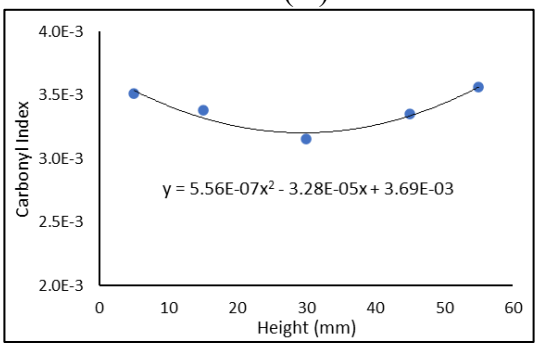

(o)

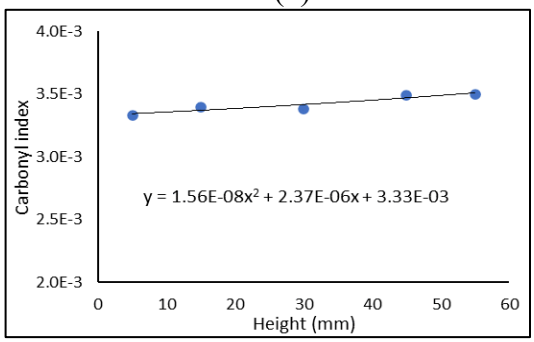

(p)

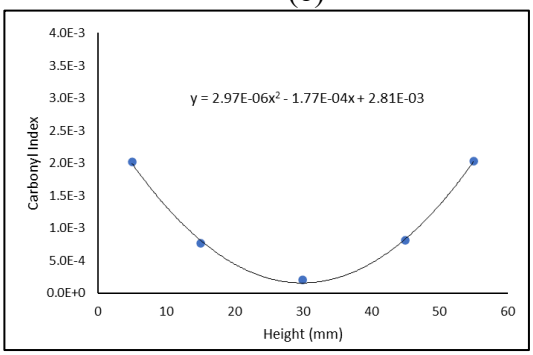

(q)

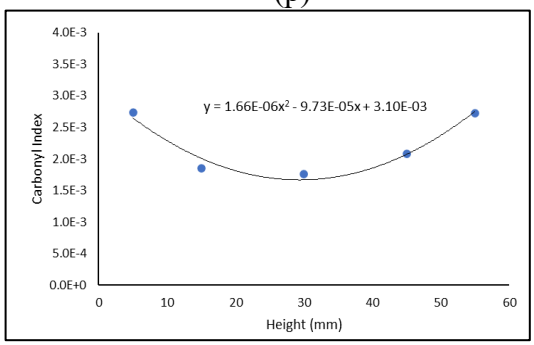

(r)

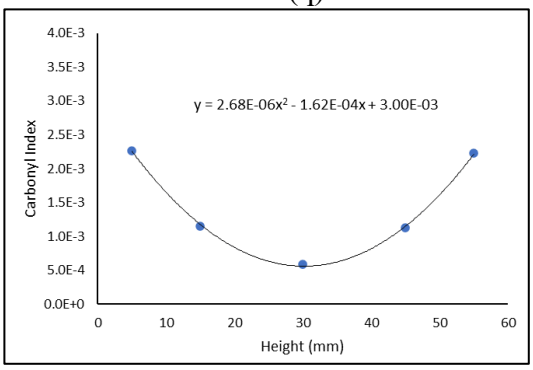

(s)

Figure. 10 Distribution of carbonyl index in different layers for WC-10: (a) WC-10-1; (b) WC-10-2; (c) WC-10-3; (d) WC-10-4; (e) WC-10-5; (f) WC-20-2; (g) WC-20-3; (h) WC-20-4; (i) WC-20-5; (j) WC-

20-6; (k) BC-28-1; (l) BC-28-2; (m) BC-28-3; (n) BC-28-4; (o) BC-28-5; (p) BC-28-6; (q) SMA-20-2; (r) SMA-20-3; (s) SMA-20-4

In Fig. 10, most of the specimens exhibit an approximately symmetrical distribution of the carbonyl index. A quadratic function appears to fit the data very well. The coefficient of the second-degree terms in the quadratic function controls the degree of curvature of the graph. Steeper curvature corresponds to greater aging gradient along the mixture specimen, indicating the capacity of the mixture against oxygen diffusion (or aging resistant capacity). Therefore, the coefficient of the second-degree term in the quadratic function is designated as Δ_{aging} to represent the aging gradient of the asphalt mixture specimens. Δ_{aging} indicates the aging susceptibility of an asphalt mixture. The surface of a mixture sample can be more easily oxidized because it is close to the atmosphere. If a mixture has low aging susceptibility, the inner part of the mixture would be better "protected" away from oxidation. Conversely, a mixture with high aging susceptibility would age more in the inner part. In the extreme case, the most aging-susceptible mixture would age uniformly throughout the mixture. Therefore, Δ_{aging} is a good indicator to represent the aging susceptibility of the mixture.

Fig. 11 shows the relationship between Δ_{aging} and the AV content. As shown in the figure, for asphalt mixture samples of the same gradation, the aging gradient decreases with the increase of AV content. When AV content exceeds a certain value, however, the aging difference in different layers of the mixture specimens is much reduced. For example, specimen BC-28-6 has the highest AV content among the BC-28 specimens, and the aging gradient in BC-28-6 is negligible. However, for different asphalt mixtures, there is no direct relationship between Δ_{aging} and the AV content. For instance, SMA-20-2 has the same AV content as BC-28-5, but the aging gradient of SMA-20-2 is much greater than that of BC-28-5.

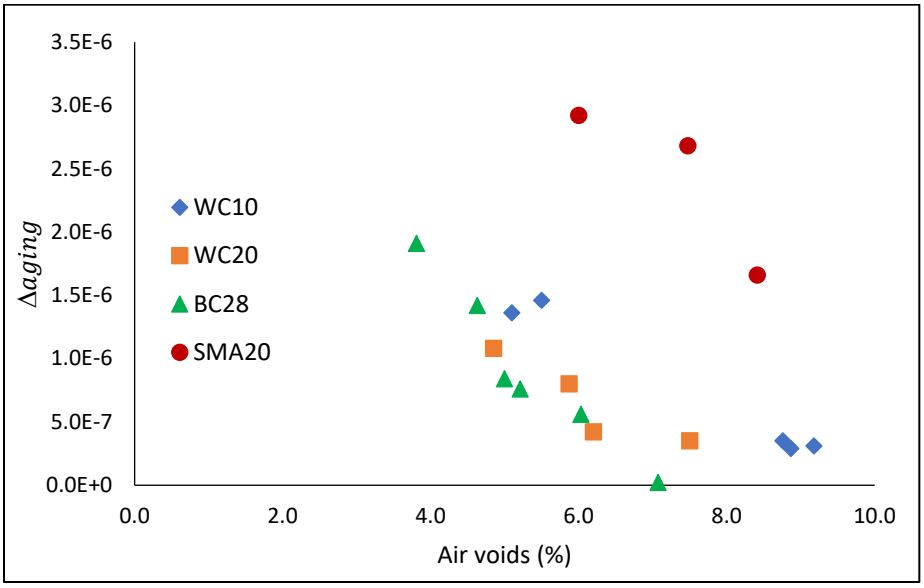

Figure 11. Δ_{aging} and the AV content.

The relationship between Δ_{aging} and *Ds* is shown in Fig. 12. Clearly, as compared to air voids, *Ds* is more closely related to Δ_{aging} , which decreases with the increase of *Ds*. The overall trend can be well captured by a log-linear model, as shown in Fig. 13. The high R^2 value indicates the relationship between Δ_{aging} and *Ds* can be universally applied to different mixture types, unlike the relationship between Δ_{aging} and

AV content. Therefore, *Ds* may serve as a valuable and convenient index to evaluate and predict the aging gradient of an asphalt mixture, which is related to the mixture's aging susceptibility. The well-fit relationship between Δ_{aging} and *Ds* is not surprising, as *Ds* fundamentally determines the efficiency of oxygen transport into inner asphalt mixtures.

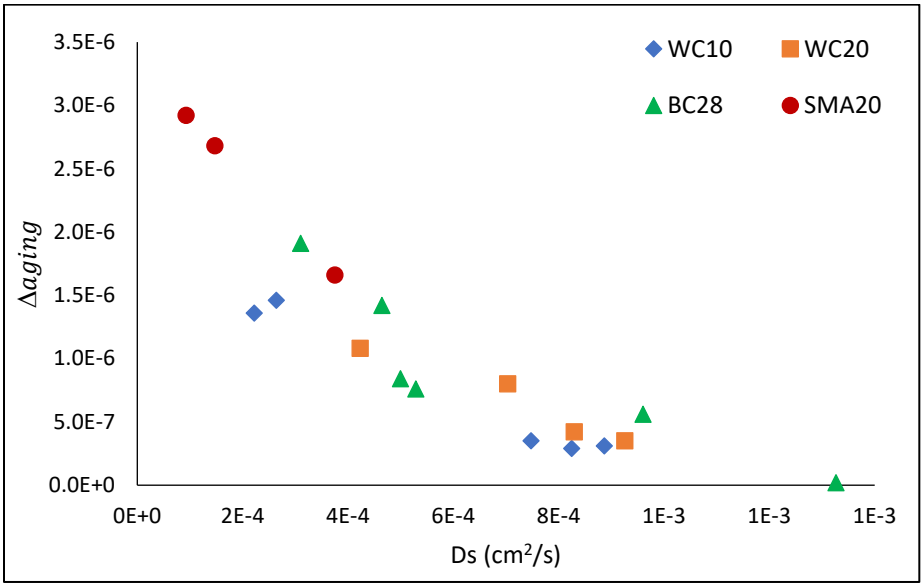

Figure 12. Δ_{aging} and the *Ds*

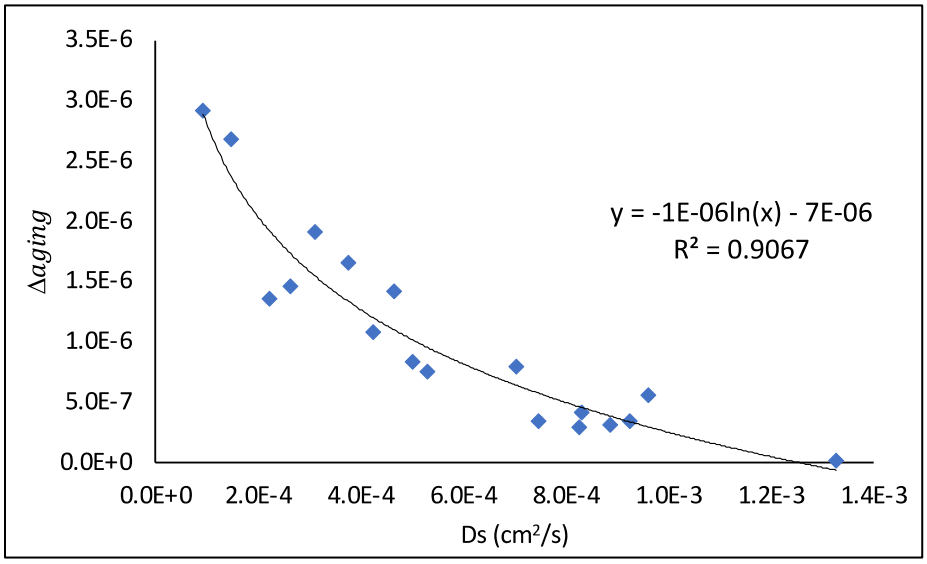

Figure 13. Regression results for Δ_{aging} and *Ds*

4.3 *Ds* and the aging severity of asphalt mixtures

Figure 14 (a)~(e) shows the relationships between *Ds* and the aging severity of asphalt binders extracted from the different layers of the mixture samples. Note that the thickness of each layer is 10 mm except for the middle layer, which is 20 mm. The figure indicates that correlations between *Ds* and aging severity for binders from layer-two, layer-three, and layer-four range are quite strong, but the correlations are not as strong for layer-one and layer-five. This is reasonable because the top and bottom layers have close contact with oxygen in the air, while oxidation in the middle layers highly depends on the efficiency of oxygen transport of the mixtures. This further proves that the oxygen transportation efficiency can be well characterized by *Ds*. The closer the asphalt binder approaches the middle layer of the compacted mixtures, the higher the correlations between *Ds* and binder aging severity. Moreover, the aging of asphalt even 10 mm beneath the surface is significantly affected by *Ds*. To exclude the influences of the surface (both top and bottom) layers, the average carbonyl index for binders from layer-two, layer-three, layer-four is calculated and used to represent the overall aging severity of the mixtures. The relationship between *Ds* and the overall aging severity is shown in Figure 14 (f). The high R^2 value implies that *Ds* is indeed appropriate to characterize the overall aging susceptibility of asphalt mixtures.

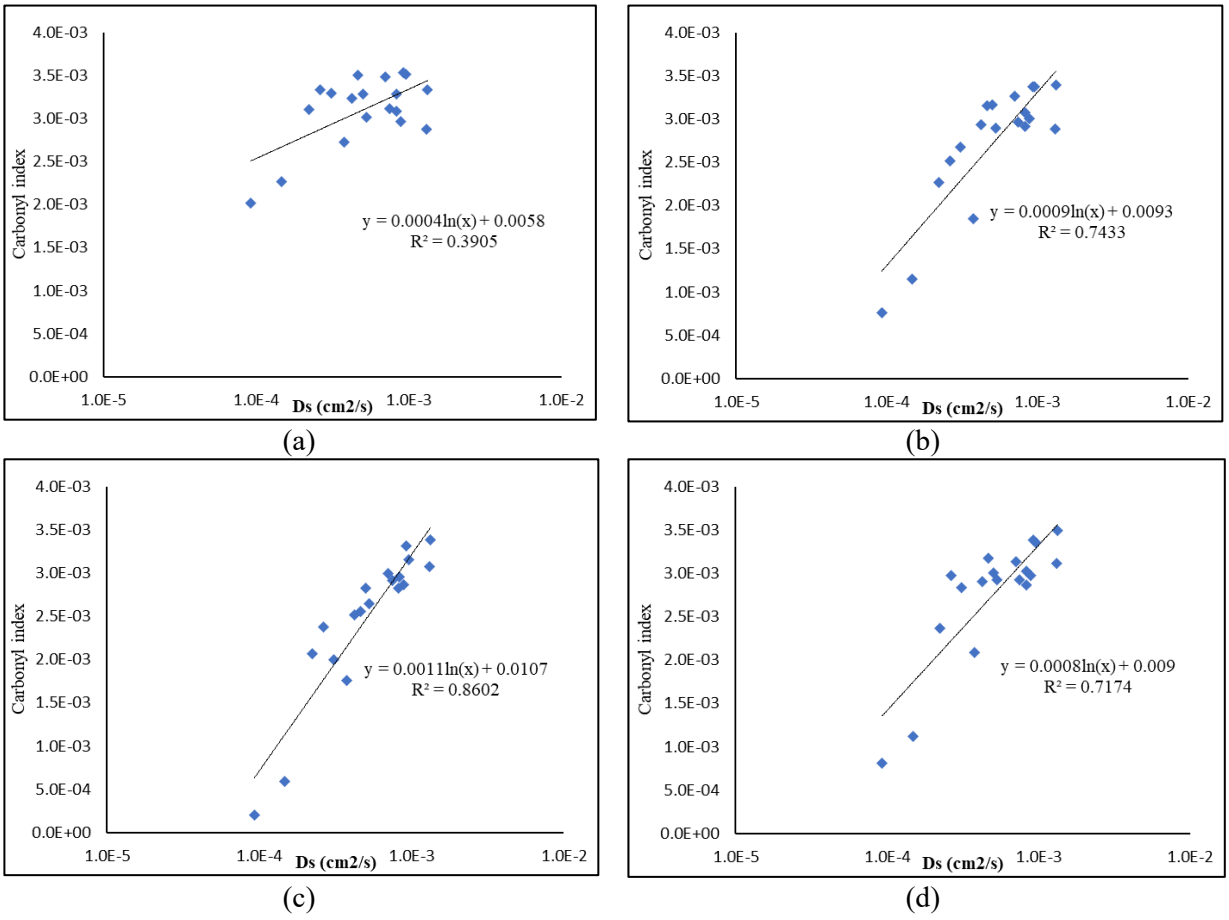

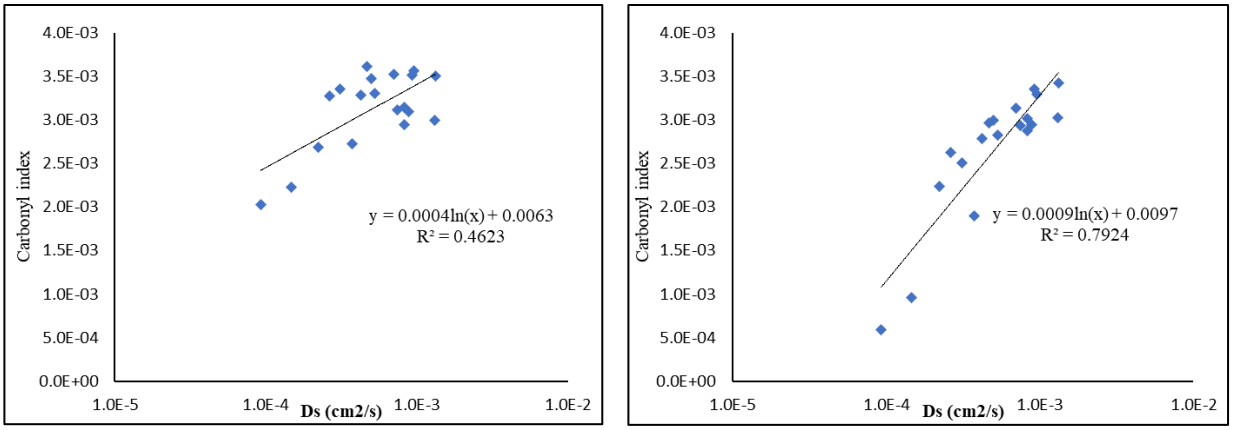

(e) (f)

Figure 14. *Ds* and aging severity in different layers: (a) layer-one; (b) layer-two; (c) layer-three; (d) layer-four; (e) layer-five; (f) *Ds* and average aging severity for layer-two, layer-three, and layer-four

For comparison purposes, Figure 15 shows the effect of AVs on the aging of asphalt mixtures. Small R^2 values in Fig. 15 indicate that there are no direct relationships between AVs and aging for asphalt mixtures. Therefore, *Ds* is a more suitable parameter than AVs to characterize the aging of asphalt mixtures.

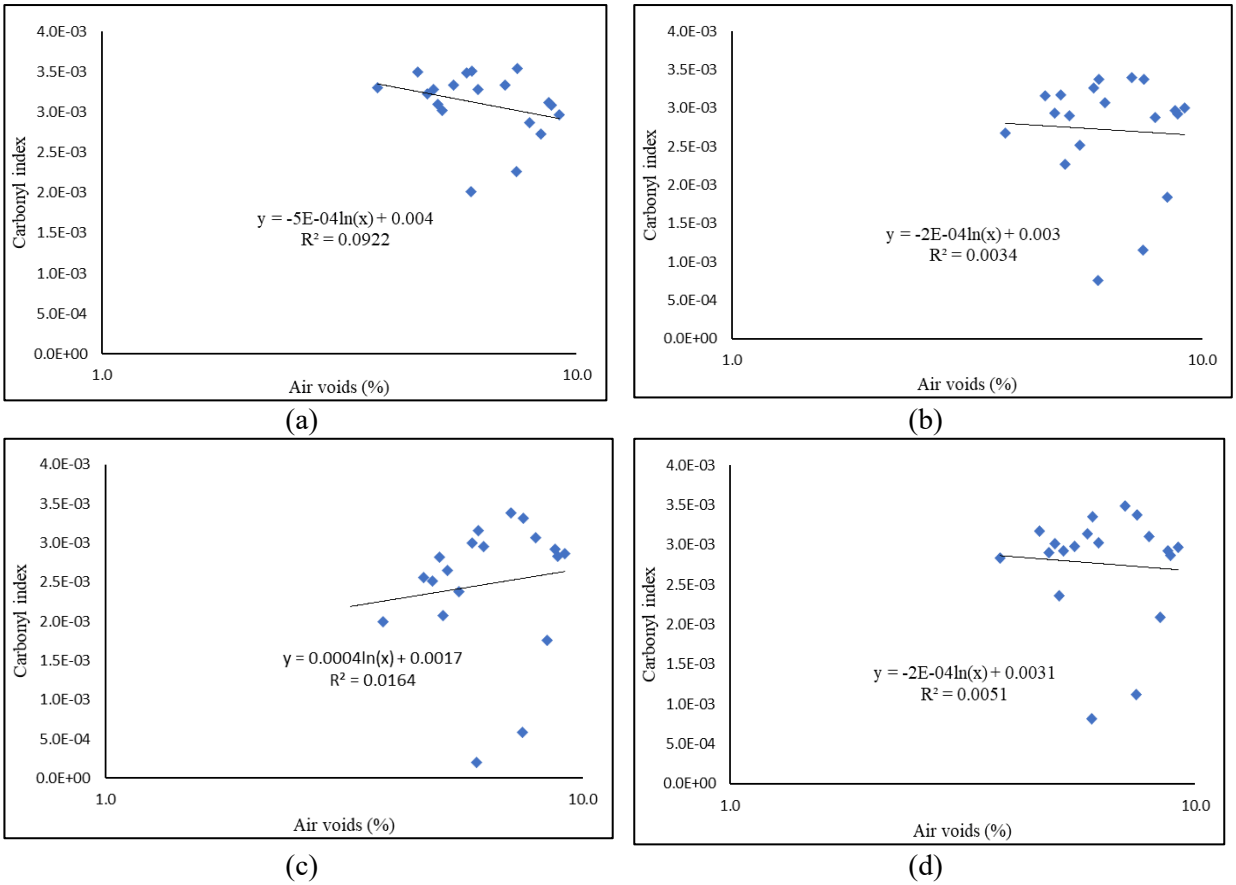

(a) (b)

(c) (d)

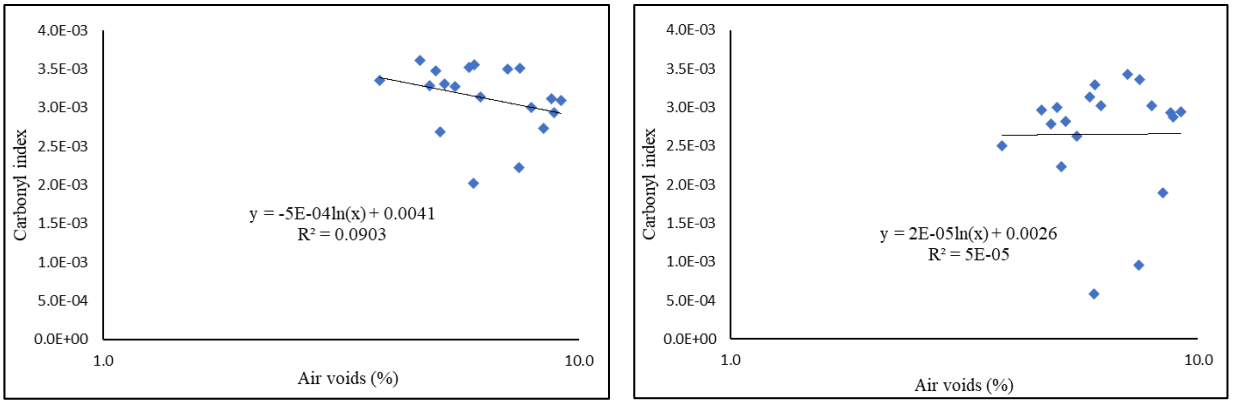

Figure 15. AVs and the aging severity in different layers: (a) layer-one; (b) layer-two; (c) layer-three; (d) layer-four; (e) layer-five; (f) *Ds* and average aging severity for layer-two, layer-three, and layer-four

5. Conclusion and Recommendation

An upgraded diffusion test apparatus was developed to determine the diffusion coefficient (*Ds*) of asphalt mixtures with different gradations and air voids (AVs). The same asphalt mixture samples were subsequently subjected to one-dimensional long-term aging treatments. Asphalt binders from different slices of the aged specimens were extracted and recovered, and their aging states were determined using FTIR. Influences of *Ds* and AV content on binder aging gradients in the asphalt mixture were systematically examined. The following conclusions are drawn from the test and analysis results.

(1) The *Ds* values of asphalt mixtures are influenced by mixtures' volumetric characteristics including gradation, AV content, and the nominal maximum aggregate size. It is a comprehensive indicator of the oxygen transportation efficiency of compacted asphalt mixtures.
(2) The majority of the asphalt mixture samples subjected to aging treatment demonstrate a similar pattern of the aging gradient along the depth profile. Asphalt binders in the top and bottom surface layers of the mixture samples are more severely aged than those in the middle layers.
(3) For each mixture type, the aging gradients of asphalt binders in the mixture samples are closely related to AV contents. Such a relationship, however, is specific to mixture type. On the other hand, the *Ds* values are closely and universally related to the aging gradients of all asphalt mixture types.
(4) The aging extent of asphalt binder in the inner portion of an asphalt mixture is closely related to the *Ds* value of the mixture. In view of the close relationships between *Ds* and aging gradient and between *Ds* and aging severity of asphalt mixtures, the *Ds* value of an asphalt mixture may serve as a useful surrogate to assess the aging susceptibility of the asphalt mixture. The determination of *Ds* does not demand expensive equipment and complicated test procedure. Therefore, it can serve as a promising parameter in designing more aging-resistant mixtures, modeling and predicting field pavement aging.

Since testing the *Ds* of asphalt mixture to evaluate its aging susceptibility is newly proposed, additional studies may be performed in the future to gain more understanding on this parameter. In particular, the following research directions are recommended:

(1) The rheological properties of the extracted asphalt binders at different depth may be further tested to evaluate the influences of aging difference on binder rheology. This will facilitate easier interpretation on the test results and better connection to industry practices.

(2) Asphalt binder aging is also dependent on binder type. The aging susceptibility of an asphalt binder is governed by the oxidation kinetics of the specific binder. The relative impacts of binder's aging susceptibility and *Ds* may be evaluated and compared.
(3) In this study, only air voids content is used as the independent variable to model *Ds* for each type of mixture of a same gradation. Other volumetric properties such as the VMA and VFA may be also considered in modeling *Ds*."
(4) The concept and method of determining *Ds* may be applied to the preventative maintenance of asphalt pavements. Impeding oxygen diffusion is one of the strategies in preventative maintenance to retard pavement aging. Since D_s reflects the oxygen transport efficiency of asphalt mixtures, it may be used to evaluate the effectiveness of preventative maintenance measures on reducing oxygen diffusion.

Acknowledgments

The research was supported by the grant (Project No. PolyU 15208518) funded by the Research Grants Council of Hong Kong Special Administrative Region Government, the grant (Grant No. 51908056) from the National Natural Science Foundation of China, and the grant (Grant No. 2019M653521) from China Postdoctoral Science Foundation.

Author Contributions

The authors confirm contribution to the papers as follows: study conception and design: Yuhong Wang; data collection: Xingyu Chen; analysis and interpretation of results: Xingyu Chen, Yong Wen; draft manuscript preparation: Xingyu Chen, Yuhong Wang, Huailei Cheng, Gengren Hao. All authors reviewed the results and approved the final version of the manuscript.

Declaration of Conflicting Interests

The authors declared no potential conflicts of interest with respect to the research, authorship, and/or publication of this article.

Reference

1. Petersen J.C. 2009. A review of the fundamentals of asphalt oxidation – chemical, physicochemical, physical property and durability relationships, No. E-C140, *Transportation Research Board*, Washington, D.C.
2. Wang, Y., Wen, Y., Zhao, K., Chong, D. and Wei, J., 2014. Connections between the rheological and chemical properties of long-term aged asphalt binders. *ASCE Journal of Materials in Civil Engineering, 27(9)*, p.04014248.
3. Luo, X., Gu, F., & Lytton, R. L. (2019). Kinetics-based aging prediction of asphalt mixtures using field deflection data. *International Journal of Pavement Engineering, 20(3),* 287-297.
4. Morian, N., Hajj, E. Y., Glover, C. J., & Sebaaly, P. E. (2011). Oxidative aging of asphalt binders in hot-mix asphalt mixtures. *Transportation research record*, *2207*(1), 107-116.
5. Wen, Y., & Wang, Y. (2019). Effect of oxidative aging on dynamic modulus of hot-mix asphalt mixtures. *Journal of Materials in Civil Engineering, 31(1),* 04018348.

6. Sun, Y., Huang B., J. Chen, X. Jia, and Y. Ding, 2016. Characterizing rheological behavior of asphalt binder over as complete range of pavement service loading frequency and temperature," Construction & Building Materials, Vol. 123: 661–672.
7. Chen, J.S., Huang, L.S., 2000. Developing an aging model to evaluate engineering properties of asphalt paving binders. Materials and Structures, 33(9): 559-565.
8. Petersen JC, Robertson RE, Branthaver JF, Harnsberger PM, Duvall JJ, Kim SS, Anderson DA, Christiansen DW, HU B. 1994. Binder characterization and evaluation, vol. 1: physical characterization. Strategic Highway Research Program (SHRP), SHRP Report no.: SHRP-A-367. Washington, D.C.
9. Kim, Y. R., Castorena, C., Elwardany, M. D., Rad, F. Y., Underwood, S., Akshay, G., ... & Glaser, R. R. (2018). Long-term aging of asphalt mixtures for performance testing and prediction.
10. Coons, R. F. (1965). An investigation of the hardening of asphalt recovered from pavements of various ages (Doctoral dissertation, Georgia Institute of Technology).
11. Mirza, M. W. (1993). Development of a global aging system for short and long term aging of asphalt cements (Doctoral dissertation, University of Maryland, College Park).
12. Glover, C. J., Davison, R. R., Domke, C. H., Ruan, Y., Juristyarini, P., Knorr, D. B., & Jung, S. H. (2005). Development of a new method for assessing asphalt binder durability with field validation. Texas Dept Transport, 1872, 1-334.
13. Al-Azri, N. A., Jung, S. H., Lunsford, K. M., Ferry, A., Bullin, J. A., Davison, R. R., & Glover, C. J. (2006). Binder oxidative aging in Texas pavements: Hardening rates, hardening susceptibilities, and impact of pavement depth. Transportation research record, 1962(1), 12-20.
14. Glover, C. J., Liu, G., Rose, A. A., Tong, Y., Gu, F., Ling, M., ... & Lytton, R. L. (2014). Evaluation of binder aging and its influence in aging of hot mix asphalt concrete (No. FHWA/TX-14/0-6613-1).
15. Wang, Y., Wong, A. S., Wen, Y., Chen, L., Chong, D., & Wang, H. (2016). Characterization of the distress modes and in situ material properties of highway asphalt pavement with long service life. Journal of Performance of Constructed Facilities, 30(4), 04015095.
16. Glover, C. J., Martin, A. E., Chowdhury, A., Han, R., Prapaitrakul, N., Jin, X., & Lawrence, J. (2009). Evaluation of binder aging and its influence in aging of hot mix asphalt concrete: literature review and experimental design.
17. Han R. 2011. Improvement to a transport model of asphalt binder oxidation in pavements: pavement temperature modeling, oxygen diffusivity in asphalt binders and mastics, & pavement air void characterization. Ph.D. dissertation. Texas A&M Univ.
18. Rose, A. A. 2016. Pavement air void property determination and incorporation of pavement air void properties in pavement oxidation modeling with an emphasis on X-Ray CT image analysis. Ph.D. dissertation. Texas A&M Univ.
19. Prapaitrakul, N, Han, R, Jin, X, Glover, CJ. 2009. A transport model of asphalt binder oxidation in pavements. Rd Materials & Pavement Design. 10/SI: 95-113.
20. Prapaitrakul, N. 2009. Towards an improved model of asphalt binder oxidation in pavements. Ph.D. Dissertation, 2009. Texas A&M, College Station, TX.
21. Han, R., Jin, X. and Glover, C.J., 2013. Oxygen diffusivity in asphalts and mastics. Petroleum Science and Technology, 31(15), pp.1563-1573.
22. Jin, X., Cui, Y. and Glover, C.J., 2013. Modeling asphalt oxidation in pavement with field validation. Petroleum science and technology, 31(13), pp.1398-1405.
23. Das, P.K., Birgisson, B., Jelagin, D. and Kringos, N., 2015. Investigation of the asphalt mixture morphology influence on its ageing susceptibility. Materials and Structures, 48(4), pp.987-1000.
24. Ling C., Wang Y. 2017. Improved image unevenness reduction and thresholding methods for effective asphalt X-Ray CT image segmentation, ASCE J. of Computing in Civil Engineering, Vol. 31. https://doi.org/10.1061/(ASCE)CP.1943-5487.0000631

25. Wang L. 2011. Mechanics of asphalt: microstructure and micromechanics, 1st ed., McGraw-Hill, New York.
26. Wang, P. Y., Wen, Y., Zhao, K., Chong, D., & Wong, A. S. (2014). Evolution and locational variation of asphalt binder aging in long-life hot-mix asphalt pavements. Construction and building materials, 68, 172-182.
27. Fini, A., Frangi, P., Robbiani, E., & Ferrini, F. (2016). Pervious vs. impervious pavements for sidewalks: effects on soil characteristics and physiology of two establishing urban tree species. ISA-Arbor. com.
28. Wen, Y., & Wang, Y. (2018). Determination of oxygen diffusion coefficients of compacted asphalt mixtures. Construction and Building Materials, 160, 385-398.
29. Sallam A., Jury W., Letey J. 1984. Measurement of gas diffusion coefficient under relatively low air-filled porosity, Soil Science Society of America Journal 48(1): 3-6.
30. Jones S.B., Or D., Bingham G.E. 2003. Gas diffusion measurement and modeling in coarse-textured porous media, Vadose Zone Journal 2(4): 602-610.
31. Asphalt Institute. (2014). MS-2 asphalt mix design methods. Asphalt Institute.
32. Petersen, J.C. and Harnsberger, P.M. 1998. Asphalt aging dual oxidation mechanism and its interrelationships with asphalt composition and oxidation age hardening, Transportation Research Record, Vol. 1638: 47-55.
33. Petersen, J.C., Branthaver, J.F., Robertson, R.E., Harnsberger, P.M., Duvall, J.J. and Ensley, E.K., 1993. Effects of physicochemical factors on asphalt oxidation kinetics. Transportation Research Record, (1391).
34. Yang, X., You, Z. and Mills-Beale, J., 2015. Asphalt binders blended with a high percentage of biobinders: Aging mechanism using FTIR and rheology. Journal of Materials in Civil Engineering, 27(4), p.04014157.
35. Yut, I. and Zofka, A., 2011. Attenuated total reflection (ATR) Fourier transform infrared (FT-IR) spectroscopy of oxidized polymer-modified bitumens. Applied Spectroscopy, 65(7), pp.765-770.
36. Lamontagne, J., Dumas, P., Mouillet, V. and Kister, J., 2001. Comparison by Fourier transform infrared (FTIR) spectroscopy of different ageing techniques: application to road bitumens. Fuel, 80(4), pp.483-488.